

BIFURCATION ANALYSIS OF A CLASS OF PLANAR PIECEWISE SMOOTH LINEAR-QUADRATIC SYSTEM^{*†}

Qiwen Xiu, Dingheng Pi[‡]

(Fujian Province University Key Laboratory of Computational Science, School of
Mathematical Sciences, Huaqiao University, Quanzhou 362021, Fujian, PR China)

Abstract

In this paper, we consider a planar piecewise smooth differential system consisting of a linear system and a quadratic Hamiltonian system. The quadratic system has some folds on the discontinuity line. The linear system may have a focus, saddle or node. Our results show that this piecewise smooth differential system will have two limit cycles and a sliding cycle. Moreover, this piecewise smooth system will undergo pseudo-homoclinic bifurcation, Hopf bifurcation and critical crossing bifurcation *CC*. Some examples are given to illustrate our results.

Keywords piecewise smooth systems; limit cycle; sliding cycle; pseudo-homoclinic bifurcation; critical crossing bifurcation *CC*

2000 Mathematics Subject Classification 34A36

1 Introduction

The bifurcation theory of planar smooth differential systems has developed very fast since D. Hilbert put up the famous Hilbert's 16th problem (see e.g. [19] and [23]). In recent years, piecewise smooth (PWS for short) dynamical systems with some parameters have been widely applied in many fields, such as mechanics, electronics, control theory, biology, economy and so on. They are also used to explain some phenomena such as pest control or model some mechanical systems exhibiting dry

^{*}The first author was partially supported by Postgraduate research and innovation ability cultivation plan of Huaqiao University. The second author was partially supported by NNSF of China grant11671040, Cultivation Program for Outstanding Young Scientific talents of Fujian Province in 2017, Program for Innovative Research Team in Science and Technology in Fujian Province University, Quanzhou High-Level Talents Support Plan under Grant 2017ZT012 and Promotion Program for Young and Middle-aged Teacher in Science and Technology Research of Huaqiao University (ZQN-YX401).

[†]Manuscript received April 28, 2020

[‡]Corresponding author. E-mail: pidh@hqu.edu.cn

friction and electrical circuits having switches and so on. These wide applications and study of Hilbert’s 16th problem are important sources of motivation of bifurcation analysis in PWS systems (see e.g. [7,16,20,30-32]).

Filippov established some systematic methods to study qualitative theory of PWS systems in his book [9]. Kuznetsov et al. studied one-parameter bifurcations in planar Filippov systems. They gave an overview of all codimension one bifurcations including some novel bifurcation phenomena that can only appear in planar PWS systems in [21]. Guardia et al. studied local and global bifurcation in PWS systems in [14]. Many novel bifurcation phenomena that will not be seen in smooth systems have been hot issues of bifurcation problems of PWS systems such as sliding bifurcation, critical crossing cycle bifurcation and so on. Freire et al. studied critical crossing cycle bifurcation and pointed out that critical crossing cycle bifurcation CC can occur in co-dimension one bifurcation, but critical crossing cycle bifurcation CC_2 cannot occur in co-dimension one bifurcation problems (see [12]).

When subsystems of planar PWS systems have the same type of singularities and different types of singularities, their bifurcation problems have been widely studied in the past few years. Even for planar PWS linear systems defined in two zones, their bifurcation problems are not easy to be studied. People have found many novel bifurcation phenomena that will not appear in smooth linear systems (see [13,15]). It is not easy for people to discuss bifurcation phenomena of planar piecewise linear systems with many parameters. Luckily, Freire et al. gave a Liénard-like canonical form for a class of piecewise linear systems with two zones. When each subsystem has no equilibrium point in its own zone and if each subsystem has a focus, they showed that two limit cycles can exist (see e.g. [10]). PWS linear systems with node-node dynamics and saddle-saddle types were considered in [17] and [18], respectively.

Recently, bifurcation phenomena of planar PWS systems that are constituted by linear system and quadratic Hamiltonian system have been studied by some authors (see e.g. [22,27-29]).

Li and Huang [22] considered the following PWS system

$$(\dot{u}, \dot{v}) = \begin{cases} (a_0 + \eta, b_1^+ u + b_2^+ u^2 + \epsilon^+), & \text{if } v > 0, \\ (-a_0 + a_1^- u + a_2^- v - \eta, b_1^- u + \epsilon^-), & \text{if } v < 0. \end{cases} \quad (1)$$

Under their assumptions, the linear system has a saddle. They got the following system which is topologically equivalent to system (1)

$$(\dot{x}, \dot{y}) = \begin{cases} (1, -2x + 3lx^2 + \epsilon_1), & \text{if } y > 0, \\ (-1 + mx + ny, -x + \epsilon_2), & \text{if } y < 0. \end{cases} \quad (2)$$

The unperturbed system of (2) is the following system (3). See equation (7) in [22].

This PWS system is made up of a quadratic Hamiltonian system and a linear system

$$\begin{pmatrix} \dot{x} \\ \dot{y} \end{pmatrix} = \begin{pmatrix} F_1(x, y) \\ F_2(x, y) \end{pmatrix} \quad (3)$$

with

$$\begin{pmatrix} F_1(x, y) \\ F_2(x, y) \end{pmatrix} = \begin{pmatrix} 1 \\ -2x + 3lx^2 \end{pmatrix}, \quad \text{for } y > 0, \quad (4)$$

and

$$\begin{pmatrix} F_1(x, y) \\ F_2(x, y) \end{pmatrix} = \begin{pmatrix} -1 + mx + ny \\ -x \end{pmatrix}, \quad \text{for } y < 0, \quad (5)$$

where $l (\neq 0)$, m , n are 3 real parameters.

When the subsystem of PWS systems has a fold, many bifurcation phenomena will occur. PWS systems with 3 parameters were discussed by Buzzi et al. in [4]. They discussed a special unfolding for PWS systems having a fold-cusp singularity. System (4) also has some folds (that is tangency points of second order). The definition of fold and cusp can be found in [14] (see Definition 2.1).

Li and Huang [22] assumed that these parameters satisfy some conditions, then the linear system has a saddle and its quadratic system has some folds. They discussed the homoclinic bifurcation of system (3). Moreover, they discussed Hopf bifurcation for a perturbed system of system (3). For more general scenarios, the stability and perturbations of generalized loops of planar PWS systems have been studied by applying Melnikov function. The loop has a saddle and a tangency point (see Figure 1 of [5]). Limit cycles bifurcating from generalized homoclinic loops having a tangent points were studied by analyzing Poincaré map and the authors found at most two limit cycles can appear in the related planar PWS systems (see [24]). Under the assumption that there exists a family of periodic orbits on the inner (resp., outer) side of the homoclinic loop, Liang and his collaborators studied homoclinic bifurcations of planar PWS systems with a generalized homoclinic loop having a saddle-fold point by analyzing the asymptotic expansion of the first order Melnikov function corresponding to the period annulus in [25].

As the parameters vary, the linear system of (1) will have a focus or a node. We can still have similar form as given by system (2). To our knowledge, when one subsystem has a fold and the other subsystem has a focus or a node, we still know little on their bifurcation phenomena. However, Li did not consider these scenarios in [22]. A natural question is: Does system (2) have other bifurcation phenomena when its linear subsystem has a node or a focus? This problem deserves to be further studied. Indeed, we find some interesting bifurcation phenomena in this paper.

In this paper we shall first investigate bifurcation phenomena of the unperturbed system (3). In the sequel, we study bifurcation phenomena of system (2). At this

moment, the linear system (5) has a focus or a node. Let $\Sigma = \{(x, 0) | x \in R\}$. In what follows we call equation (3) with (4) the upper system of (3) and equation (3) with (5) the lower system of (3). We denote upper system and lower system of (3) by $f^+(x, y)$ and $f^-(x, y)$, respectively. Our results will show that when the linear system (5) has a focus or a node, system (3) has a sliding cycle and undergoes pseudo-homoclinic bifurcation and critical crossing bifurcation CC . These novel bifurcation phenomena will not appear in smooth planar differential systems.

From [21] (see P2171), we know that one can construct a local transversal section to a stable sliding cycle and define Poincaré map in the usual way forward in time. Note that all nearby points will be mapped into the fixed point of Poincaré map, the derivative of Poincaré map at the fixed point corresponding to the sliding cycle will be zero. This is referred to as superstability. In this case Poincaré map is not invertible. However, a generic crossing cycle has a smooth invertible Poincaré map. We often use the derivative of Poincaré map to discuss the stability of a crossing cycle. If the derivative μ of Poincaré map satisfies $\mu < 1$, the crossing cycle is exponentially stable. If the derivative μ of Poincaré map satisfies $\mu > 1$, the crossing cycle is exponentially unstable. A crossing critical cycle is a crossing cycle passing through the boundary of a sliding segment. The crossing critical cycle is the intermediate situation between a sliding cycle and a crossing cycle.

We recall definitions of critical crossing cycle bifurcations CC and CC_2 for the sake of completeness (see [12] and [21]). When planar PWS systems with parameter α undergo critical crossing bifurcation CC , there is a sliding cycle with a single sliding segment ending at a tangency point when the parameter $\alpha < 0$. This sliding segment shrinks for $\alpha \rightarrow 0$. The sliding cycle becomes a crossing critical cycle when $\alpha = 0$. Then the critical crossing cycle disappears for $\alpha > 0$ forming an exponentially stable crossing limit cycle. See CC of Figure 17 in [21].

When planar PWS systems with the parameter α undergo *critical crossing bifurcation* CC_2 , a superstable sliding cycle coexists with an exponentially unstable crossing cycle for sufficiently small parameter $\alpha < 0$. The two cycles collide at $\alpha = 0$ forming a critical crossing cycle and then disappear for $\alpha > 0$. This bifurcation implies the catastrophic disappearance of a stable sliding cycle.

This paper is organized as follows. In Section 2 we will state our main results. Their proofs will be given in Section 3. Some examples will be given to apply our results in Section 4. We give our conclusions in Section 5.

2 Statement of the Main Results

Before we state our main results, we need some basic facts on the upper and lower systems of (3). The orbits of upper system (4) are some cubic curves

$$y = -x^2 + lx^3 + c, \quad \text{for } c \geq 0. \tag{6}$$

The upper half system of (3) has two folds on Σ , that is, the origin $O(0, 0)$ and point $B = (\frac{2}{3l}, 0)$. Moreover, the point B is visible and the point O is invisible. Its orbit passing through the point B will have another intersection point with Σ , denoted by \bar{B} . We substitute the coordinates of the point B into equation (6), we get that $c = \frac{4}{27l^2}$. So the expression of the orbit that goes through the point B is

$$y = -x^2 + lx^3 + \frac{4}{27l^2}. \tag{7}$$

Let $-x^2 + lx^3 + \frac{4}{27l^2} = 0$, and factor the left-hand side, we have

$$-x^2 + lx^3 + \frac{4}{27l^2} = l \cdot \left(x - \frac{2}{3l}\right)^2 \left(x + \frac{1}{3l}\right) = 0. \tag{8}$$

Thus we get that $\bar{B} = (-\frac{1}{3l}, 0)$. Based on the analysis of system (4), we know that when $l < 0$ the orbits starting at point $(x_0, 0)$ with $x_0 \in [\frac{2}{3l}, 0]$ will enter the upper half-plane under the action of the flows of the upper subsystem. These orbits will reach Σ again at some point $(x_1, 0)$ with $x_1 \in [0, -\frac{1}{3l}]$, after certain time $t > 0$. Analogously, if $l > 0$ the orbits starting at point $(x_0, 0)$ with $x_0 \in [-\frac{1}{3l}, 0]$ will go into the upper half-plane under the action of the flows of the upper subsystem. These orbits can reach Σ again at some points $(x_1, 0)$ with $x_1 \in [0, \frac{2}{3l}]$, after certain time $t > 0$. We define a upper Poincaré map P_+ as $x_1 = P_+(x_0)$ with $P_+(0) = 0$. Solving the upper system (4) gives

$$0 = -x_1^2 + lx_1^3 + x_0^2 - lx_0^3. \tag{9}$$

If system (3) has a closed cycle (except sliding closed cycle), it must intersect Σ and is located between B and \bar{B} . The following lemma will be used in the proof of our main results (see [9]).

Lemma 1 *Consider the equation*

$$\frac{dy}{dx} = ax + by + G(x, y), \quad a \neq 0, \tag{10}$$

where G is of class C^4 at the origin satisfying

$$G(x, y) = cx^2 + dxy + ey^2 + fx^3 + gx^2y + hx^4 + o(x^4 + y^2),$$

for (x, y) near the origin. Let $y = Y(x)$ be the solution of (10) satisfying

$$Y(-r) = Y(\sigma) = 0, \quad -r < x < 0, \quad \text{and} \quad aY(x) < 0 \quad \text{for} \quad -r < x < 0,$$

then for small enough $r > 0$

$$\sigma = r + \mu r^2 + \mu^2 r^3 + kr^4 + o(r^4), \tag{11}$$

where

$$\mu = \frac{2}{3}\left(b - \frac{c}{a}\right), \quad k = \frac{11}{10}\mu^3 + \frac{\mu}{5}d + \frac{2}{15}L, \quad L = \frac{bc^2}{a^2} - \frac{2c^3}{a^3} - 2ae - \frac{2bf}{a} + \frac{5cf}{a^2} + g - \frac{3h}{a}.$$

For the upper Poincaré map P_+ , we have the following results.

Proposition 1 Suppose that $l \neq 0$, then the following statements hold.

(1) Define $P_+(0) = 0$, then P_+ is continuous at the point $x_0 = 0$. In addition, the first four derivatives of P_+ at the point $x_0 = 0$ are

$$P'_+(0) = -1, \quad P''_+(0) = 2l, \quad P'''_+(0) = -6l^2, \quad P^{(4)}_+(0) = 48l^3.$$

(2) P_+ is decreasing with respect to x_0 , and concave from below (above) if $l < 0$ ($l > 0$).

Proof (1) The upper system (4) can be rewritten as the

$$\frac{dy}{dx} = -2x + 3lx^2, \quad y > 0.$$

We get from Lemma 1 that

$$P_+(x_0) = -x_0 + \mu^+ x_0^2 - (\mu^+)^2 x_0^3 + k^+ x_0^4 + o((-x_0)^4), \quad (12)$$

for small enough $-x_0 > 0$, where

$$\mu^+ = l, \quad k^+ = 2l^3.$$

By equation (12), we have

$$\lim_{x_0 \rightarrow 0} P_+(x_0) = 0.$$

Moreover, we obtain first four derivatives of P_+ at the point $x_0 = 0$. Thus the statement (1) of Proposition 1 follows.

(2) We only need to prove the statement when $l < 0$. When $l > 0$, the statement can be proved similarly. By (9), if $l < 0$, we have

$$(x_1 - x_0)(lx_1^2 + (lx_0 - 1)x_1 + lx_0^2 - x_0) = 0, \quad (13)$$

where $x_0 \in (\frac{2}{3l}, 0)$ and $x_1 \in (0, -\frac{1}{3l})$. Let $h(x_1) = lx_1^2 + (lx_0 - 1)x_1 + lx_0^2 - x_0$, then the root of discriminant of $h(x_1)$ satisfies

$$\Delta = (lx_0 - 1)^2 - 4lx_0(lx_0 - 1) = -3lx_0\left(lx_0 - \frac{2}{3}\right) + 1 > 1 > 0,$$

for all $x_0 \in (\frac{2}{3l}, 0)$. Thus equation $h(x_1) = 0$ has the following two roots

$$x_{11} = \frac{1 - lx_0 - \sqrt{-3lx_0(lx_0 - \frac{2}{3}) + 1}}{2l}, \quad x_{12} = \frac{1 - lx_0 + \sqrt{-3lx_0(lx_0 - \frac{2}{3}) + 1}}{2l}.$$

It is clear that $x_{11} > 0$ and $x_{12} < 0$ when $l < 0$. Since $x_1 \in (0, -\frac{1}{3l})$, x_{12} should be discarded. The useful root of $h(x_1) = 0$ is

$$x_1 = x_{11} = \frac{1 - lx_0 - \sqrt{-3lx_0(lx_0 - \frac{2}{3}) + 1}}{2l} = \frac{1 - lx_0 - \sqrt{\Delta}}{2l}.$$

Since $x_1 = P_+(x_0)$, we have

$$P'_+(x_0) = x'_1 = -\frac{1}{2} + \frac{3lx_0 - 1}{2} \left[-3lx_0 \left(lx_0 - \frac{2}{3} \right) + 1 \right]^{-1/2} = \frac{3lx_0 - 1 - \sqrt{\Delta}}{2\Delta}. \tag{14}$$

Since $3lx_0 - 1 < 1$ and $(-3lx_0(lx_0 - \frac{2}{3}) + 1)^{-1/2} < 1$ for all $x_0 \in (\frac{2}{3l}, 0)$, we know that $P'_+(x_0) < 0$ and $P_+(x_0)$ is decreasing with respect to x_0 .

Easy calculation shows that

$$\begin{aligned} P''_+(x_0) &= \frac{l}{2} \left\{ 3 \left[-3lx_0 \left(lx_0 - \frac{2}{3} \right) + 1 \right]^{-1/2} + (3lx_0 - 1)^2 \left[-3lx_0 \left(lx_0 - \frac{2}{3} \right) + 1 \right]^{-3/2} \right\} \\ &= \frac{l(3\Delta + (3lx_0 - 1)^2)}{2\Delta\sqrt{\Delta}}. \end{aligned}$$

It is clear that $P''_+(x_0) < 0$ when $l < 0$. Therefore, P_+ is decreasing with respect to x_0 and concave from below. The proof is complete.

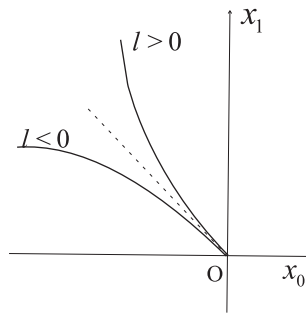


Figure 1: Graphs of the Poincaré map P_+ with different l

System (5) has a unique singularity $S = (0, \frac{1}{n})$. In what follows we will discuss the scenarios when S is a focus of the lower linear system and then S is a node of the linear system. For each scenario, we will provide a bifurcation analysis for the planar PWS system.

2.1 The lower system with focus dynamic

In this case, the singularity $S = (0, \frac{1}{n})$ of lower system is a focus. We need the assumption $n > \frac{m^2}{4}$. Let $\beta = \frac{\sqrt{4n-m^2}}{2} > 0$, the eigenvalues of $A = \begin{pmatrix} m & n \\ -1 & 0 \end{pmatrix}$ are the following

$$\lambda_1 = \frac{m}{2} + i\beta, \quad \lambda_2 = \frac{m}{2} - i\beta. \tag{15}$$

The solution of the lower system with initial value $(x_0, 0)$ at $t = 0$ is

$$\begin{aligned} x_1^-(t) &= \exp\left(\frac{m}{2}t\right)\left[x_0 \cos(\beta t) + \left(\frac{m}{2\beta}x_0 - \frac{1}{\beta}\right) \sin(\beta t)\right], \\ y_1^-(t) &= -\exp\left(\frac{m}{2}t\right)\left[\frac{1}{n} \cos(\beta t) - \left(\frac{m}{2n\beta} - \frac{x_0}{\beta}\right) \sin(\beta t)\right] + \frac{1}{n}, \end{aligned} \tag{16}$$

where $t > 0$. The orbits of lower system surrounding origin O rotate clockwise. Then the orbit of lower system starting at $(x_0, 0)$ with $x_0 > 0$, will arrive at Σ at the point $(x_1, 0)$ with $x_1 < 0$ after a certain time $t_1 > 0$. We define a lower Poincaré map P_- as $x_1 = P_-(x_0)$ with $P_-(0) = 0$. Then we have

$$y_1^-(t_1) = 0, \quad x_1^-(t_1) = x_1. \tag{17}$$

Here, we ask the $t_1 > 0$ to be minimum time such that (17) holds. Since the singularity S is not in the lower half plane, $\beta t_1 \in (0, \pi)$. It means that $\sin \beta t_1 > 0$ for $\beta t_1 \in (0, \pi)$. Therefore, we obtain the parametric representations of lower Poincaré map P_- from equations (16) and (17)

$$\begin{aligned} x_0 &= \frac{\beta e^{-\frac{m}{2}t_1}}{n \sin(\beta t_1)} \left[1 - e^{\frac{m}{2}t_1} \left(\cos(\beta t_1) - \frac{m}{2\beta} \sin(\beta t_1)\right)\right], \quad t_1 > 0, \\ x_1 &= -\frac{\beta e^{\frac{m}{2}t_1}}{n \sin(\beta t_1)} \left[1 - e^{-\frac{m}{2}t_1} \left(\cos(\beta t_1) + \frac{m}{2\beta} \sin(\beta t_1)\right)\right]. \end{aligned} \tag{18}$$

For brevity, set $s = \beta t_1$ and $\gamma = \frac{1}{2\beta} > 0$, the above two equations can be written as

$$x_0(s) = \frac{\beta e^{-m\gamma s}}{n \sin s} \varphi_{m\gamma}(s), \quad x_1(s) = -\frac{\beta e^{m\gamma s}}{n \sin s} \varphi_{-m\gamma}(s), \tag{19}$$

where $s \in (0, \pi)$, $\varphi_{m\gamma}(s) = 1 - e^{m\gamma s}(\cos s - m\gamma \sin s)$. This function has been introduced in [1] and [10]. It has the following symmetry properties

$$\varphi_{-m\gamma}(-s) = \varphi_{m\gamma}(s), \quad \varphi_{-m\gamma}(s) = \varphi_{m\gamma}(-s), \quad \text{for any } m, \gamma, s \in R.$$

Figure 2 gives the graph of $\varphi_{m\gamma}(s)$. For the lower Poincaré map P_- , we have the following proposition.

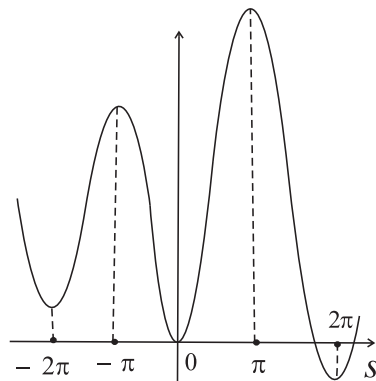


Figure 2: The graph of $\varphi_{m\gamma}(\cdot)$ for a positive value of m

Proposition 2 Suppose that system (5) satisfies the assumption $n > \frac{m^2}{4}$, $m \in R$, $s = \beta t_1$ and $\gamma = \frac{1}{2\beta}$, then the following statements hold.

(1) x_0 is increasing with respect to s and x_1 is decreasing with respect to s , with

$$\lim_{s \rightarrow 0^+} x_0(s) = \lim_{s \rightarrow 0^+} x_1(s) = 0, \quad \lim_{s \rightarrow \pi^-} x_0(s) = +\infty, \quad \lim_{s \rightarrow \pi^-} x_1(s) = -\infty.$$

(2) When $m = 0$, $P_-(x_0) = -x_0$ for all $x_0 > 0$.

(3) When $m \neq 0$, for all $x_0 > 0$, we have $P'_-(x_0) < 0$ and

$$\lim_{x_0 \rightarrow 0^+} P'_-(x_0) = -1, \quad \lim_{x_0 \rightarrow +\infty} P'_-(x_0) = -e^{m\gamma\pi}, \quad \text{sign}P''_-(x_0) = -\text{sign}m.$$

Proof It follows from (19) that

$$x'_0(s) = \frac{\beta}{n(\sin s)^2} \varphi_{-m\gamma}(s), \quad x'_1(s) = -\frac{\beta}{n(\sin s)^2} \varphi_{m\gamma}(s), \quad s \in (0, \pi). \quad (20)$$

Figure 2 and the symmetry properties of $\varphi_{m\gamma}(s)$ imply that $\varphi_{m\gamma}(s)$ and $\varphi_{-m\gamma}(s)$ are always positive when $s \in (0, \pi)$. Using the fact $n > 0$, $\beta > 0$, $x'_0(s) > 0$, we have $x'_1(s) < 0$ for $s \in (0, \pi)$. Moreover, easy calculation shows that

$$\lim_{s \rightarrow 0^+} x_0(s) = \lim_{s \rightarrow 0^+} x_1(s) = 0, \quad \lim_{s \rightarrow \pi^-} x_0(s) = +\infty, \quad \lim_{s \rightarrow \pi^-} x_1(s) = -\infty.$$

We get from (20) that

$$P'_-(x_0) = \frac{x'_1(s)}{x'_0(s)} = -\frac{\varphi_{m\gamma}(s)}{\varphi_{-m\gamma}(s)} = \frac{x_0}{P_-(x_0)} e^{2m\gamma s} < 0. \quad (21)$$

When $m = 0$, $P'_-(x_0) = -1$. By (21), $P_-(x_0) = -x_0$, for all $x_0 > 0$. When $m \neq 0$, it is clear that $P'_-(x_0) < 0$, for all $x_0 > 0$. P_- is decreasing with respect to x_0 . Furthermore,

$$\lim_{x_0 \rightarrow 0^+} P'_-(x_0) = \lim_{s \rightarrow 0^+} -\frac{\varphi_{m\gamma}(s)}{\varphi_{-m\gamma}(s)} = -1, \quad \lim_{x_0 \rightarrow +\infty} P'_-(x_0) = \lim_{s \rightarrow \pi^-} -\frac{\varphi_{m\gamma}(s)}{\varphi_{-m\gamma}(s)} = -e^{m\gamma\pi}.$$

From (21), we have

$$P''_-(x_0) = -\frac{2n^2(\sin s)^3}{\beta^3(\varphi_{-m\gamma}(s))^3} \cdot \theta(s),$$

where $\theta(s) = \sinh m\gamma s - m\gamma \sin s$. We get from $\text{sign}\theta(s) = \text{sign}m$ that $\text{sign}P''_-(x_0) = -\text{sign}m$. The proof is complete.

2.2 Sliding dynamics

In this part, we shall discuss the sliding dynamics of PWS system (3). When $l < 0$, system (3) has an attracting sliding region $\Sigma_s^- = \{(x, 0) | x \leq \frac{2}{3l}, l < 0\}$. When

$l > 0$, system (3) has a repulsive sliding region ($\Sigma_s^+ = \{(x, 0) | x \geq \frac{2}{3l}, l > 0\}$). Let $M(x, 0) \in \Sigma$, then the vector fields of upper and lower systems at point M are as follows

$$\begin{pmatrix} f_1^+(x, 0) \\ f_2^+(x, 0) \end{pmatrix} = \begin{pmatrix} 1 \\ -2x + 3lx^2 \end{pmatrix}, \quad \text{for } y = 0, \tag{22}$$

and

$$\begin{pmatrix} f_1^-(x, 0) \\ f_2^-(x, 0) \end{pmatrix} = \begin{pmatrix} -1 + mx \\ -x \end{pmatrix}, \quad \text{for } y = 0. \tag{23}$$

In fact, since the points in the sliding region must satisfy

$$f_2^+(x, 0)f_2^-(x, 0) = -x^2(3lx - 2) \leq 0.$$

It follows that the sliding regions Σ_s^- and Σ_s^+ are aforementioned. Now we establish the sliding vector field on Σ_s^- (Σ_s^+) by Filippov convex method. The sliding vector field

$$\dot{X} = \alpha f^+(X) + (1 - \alpha)f^-(X), \quad X \in \Sigma_s^-(\Sigma_s^+), \alpha \in [0, 1]$$

should be tangent to Σ , it follows that

$$\alpha(-2x + 3lx^2) + (1 - \alpha)(-x) = 0, \quad \alpha \in [0, 1].$$

Thus $\alpha = \frac{1}{3lx-1}$. The sliding vector field is given by

$$Y_s = \left(\frac{3lmx^2 - (3l + 2m)x + 3}{3lx - 1}, 0 \right).$$

In the following proposition, we will find that the sliding vector field Y_s may have a pseudo-saddle. The definition of pseudo-saddle was given in Definition 2.8 of [14].

Proposition 3 For the sliding vector field Y_s with $l < 0$, $m > 0$, there exists a unique singularity $M^- = (x_M^-, 0)$ in Σ_s^- , which is a pseudo-saddle.

Proof Set $g(x) = 3lmx^2 - (3l + 2m)x + 3$. When $l < 0$ and $m > 0$, the root of discriminant of $g(x)$ satisfies $\Delta = (3l + 2m)^2 - 36lm > 0$. Two roots of $g(x) = 0$ are the following

$$x_M^- = \frac{3l + 2m + \sqrt{(3l + 2m)^2 - 36lm}}{6lm} < 0, \quad x_M^+ = \frac{3l + 2m - \sqrt{(3l + 2m)^2 - 36lm}}{6lm} > 0.$$

Since $x_M^+ > 0 > \frac{2}{3l}$, x_M^+ is not in the interior of sliding region Σ_s^- . As for x_M^- ,

$$\begin{aligned} x_M^- - x_B &= \frac{3l + 2m + \sqrt{(3l + 2m)^2 - 36lm}}{6lm} - \frac{2}{3l} \\ &= \frac{3l - 2m + \sqrt{(3l + 2m)^2 - 36lm}}{6lm} \\ &= \frac{3l - 2m + \sqrt{(3l - 2m)^2 - 12lm}}{6lm} < 0, \end{aligned}$$

where x_B is the abscissa of point B . Since $3lx - 1 > 0$ for all $x \leq \frac{2}{3l}$, $M^- = (x_M^-, 0)$ is always on the left of point B . Moreover, Y_s has a unique singularity $M^- = (x_M^-, 0)$ in the region Σ_s^- when $l < 0$, $m > 0$. M^- is a pseudo-saddle. The proof is complete.

Analogously, we have the following results when $l > 0$ and $m < 0$.

Proposition 4 *For the sliding vector field Y_s with $l > 0$ and $m < 0$, there exists a unique singularity $M^+ = (x_M^+, 0)$ in Σ_s^+ , which is a pseudo-saddle.*

In what follows we present two main results when the lower linear system has a focus.

Theorem 1 *Suppose that system (3) satisfies the basic assumption $n > \frac{m^2}{4}$ and $l < 0$. Then the following statements hold.*

- (1) *If $m \leq 0$, system (3) has no periodic orbit.*
- (2) *If $m > 0$ and $l > -\frac{2}{3}m$, there exist l_1, l_2 satisfying $-\frac{2}{3}m < l_1 < l_2 < 0$ such that the following statements hold.*
 - (a) *If $-\frac{2}{3}m < l < l_1$, system (3) has a stable limit cycle (crossing periodic orbit).*
 - (b) *If $l = l_1$, system (3) has a stable crossing critical cycle.*
 - (c) *If $l_1 < l < l_2$, system (3) has a stable sliding cycle.*
 - (d) *If $l = l_2$, system (3) has a sliding homoclinic cycle, which is stable.*
 - (e) *If $l_2 < l < 0$, system (3) has neither periodic orbits nor sliding cycles.*
- (3) *If $m > 0$ and $l \leq -\frac{2}{3}m$, there are no corresponding l_1, l_2 that satisfy $-\infty < l_1 < l_2 < -\frac{2}{3}m$. So system (3) has no periodic orbit.*

Theorem 2 *Suppose that system (3) satisfies the basic assumption $n > \frac{m^2}{4}$ and $l > 0$. Then the following statements hold.*

- (1) *If $m \geq 0$, system (3) has no periodic orbit.*
- (2) *If $m < 0$ and $l < -\frac{2}{3}m$, then there exist l_1, l_2 satisfying $0 < l_2 < l_1 < -\frac{2}{3}m$ such that the following statements hold.*
 - (a) *If $-\frac{2}{3}m > l > l_1$, system (3) has an unstable limit cycle (crossing periodic orbit).*
 - (b) *If $l = l_1$, system (3) has an unstable crossing critical cycle.*
 - (c) *If $l_1 > l > l_2$, system (3) has an unstable sliding cycle.*
 - (d) *If $l = l_2$, system (3) has a sliding homoclinic cycle, which is unstable.*
 - (e) *If $0 < l < l_2$, system (3) has no periodic orbit.*
- (3) *If $m < 0$ and $l \geq -\frac{2}{3}m$, then there are no corresponding l_1, l_2 that satisfy $+\infty > l_1 > l_2 > -\frac{2}{3}m$. So system (3) has no periodic orbit.*

2.3 The lower linear system with node dynamics

In this section, we assume that $m^2 > 4n > 0$. S is a node of the lower linear system. Direct computation shows that

$$x_0(t) = \frac{1}{n} \cdot \frac{\Psi_{\lambda_1, \lambda_2}(t)}{e^{\lambda_1 t} - e^{\lambda_2 t}}, \quad x_1(t) = -\frac{1}{n} \cdot \frac{e^{mt} \Psi_{\lambda_1, \lambda_2}(-t)}{e^{\lambda_1 t} - e^{\lambda_2 t}}, \quad t > 0, \quad (24)$$

where λ_1, λ_2 are the eigenvalues of $A = \begin{pmatrix} m & n \\ -1 & 0 \end{pmatrix}$ and $\Psi_{\lambda_1, \lambda_2}(t) = \lambda_1 - \lambda_2 + \lambda_2 e^{\lambda_1 t} - \lambda_1 e^{\lambda_2 t}$. Let l^1 and l^2 be the invariant manifolds of lower system, then we have

$$l^1 = \left\{ (x, y) \mid y = -\frac{1}{\lambda_2}x + \frac{1}{n}, y \leq 0 \right\}, \quad l^2 = \left\{ (x, y) \mid y = -\frac{1}{\lambda_1}x + \frac{1}{n}, y \leq 0 \right\}.$$

l^1 and l^2 intersect Σ at points $A^1 = (\frac{\lambda_2}{n}, 0)$ and $A^2 = (\frac{\lambda_1}{n}, 0)$, respectively.

Proposition 5 Suppose that system (5) satisfies the assumption $m^2 > 4n > 0$ and $\lambda_1 > \lambda_2$, then the following statements hold.

- (1) $x_0(t)$ is increasing with respect to t and $x_1(t)$ is decreasing with respect to t .
- (2) When $\lambda_1 > \lambda_2 > 0$ (that is, $m > 0$), P_- given in (24) is defined on $(0, \frac{\lambda_2}{n})$ and
 - (a) P_- is decreasing and convex with respect to x_0 .
 - (b) P_- has $x_0 = \frac{\lambda_2}{n}$ as an asymptote.
- (3) When $0 > \lambda_1 > \lambda_2$ (that is, $m < 0$), P_- is defined on $(0, +\infty)$ and
 - (a) P_- is decreasing and concave with respect to x_0 .
 - (b) P_- has $x_1 = \frac{\lambda_1}{n}$ as an asymptote.
- (4) Define $P_-(0) = 0$, then P_- is continuous at the point $x_0 = 0$. In addition to this, the first four derivatives of the P_- at the point $x_0 = 0$ are

$$P'_-(0) = -1, \quad P''_-(0) = -\frac{4m}{3}, \quad P'''_-(0) = -\frac{8}{3}m^2, \quad P^{(4)}_-(0) = -\frac{16}{45}(22m^3 - 9mn).$$

Graphs of P_- for different m are shown in Figure 3.

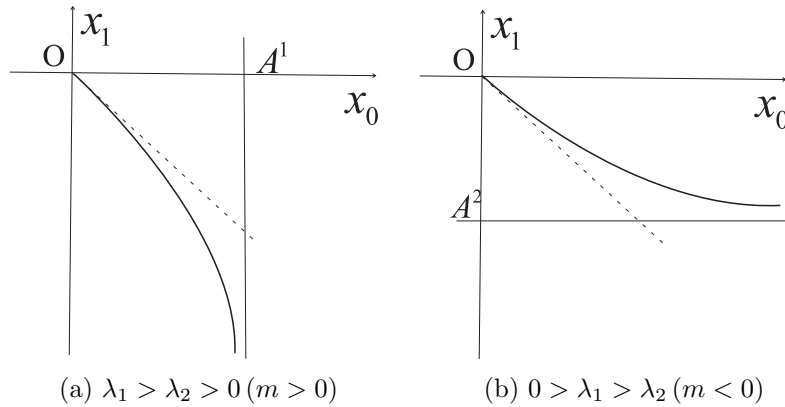


Figure 3: Graphs of the lower Poincaré map P_- for different m

Proof (1) We get from (24) that for $t > 0$

$$x'_0(t) = \frac{\lambda_1 - \lambda_2}{n} \cdot \frac{e^{mt}\Psi_{\lambda_1, \lambda_2}(-t)}{(e^{\lambda_1 t} - e^{\lambda_2 t})^2}, \quad x'_1(t) = -\frac{\lambda_1 - \lambda_2}{n} \cdot \frac{e^{mt}\Psi_{\lambda_1, \lambda_2}(t)}{(e^{\lambda_1 t} - e^{\lambda_2 t})^2}. \quad (25)$$

Since $n > 0$, $\lambda_1\lambda_2 > 0$, $\lambda_1 > \lambda_2$, we have $\Psi_{\lambda_1,\lambda_2}(t) > 0$, $\Psi_{\lambda_1,\lambda_2}(-t) > 0$. Then $x'_0(t) > 0$, $x'_1(t) < 0$ for $t > 0$. This implies that $x_0(t)$ is increasing with respect to t and $x_1(t)$ is decreasing with respect to t .

(2) When $\lambda_1 > \lambda_2 > 0$, we obtain

$$\lim_{t \rightarrow 0^+} x_0(t) = \lim_{t \rightarrow 0^+} x_1(t) = 0, \quad \lim_{t \rightarrow +\infty} x_0(t) = \frac{\lambda_2}{n}, \quad \lim_{t \rightarrow +\infty} x_1(t) = -\infty.$$

Moreover, by (25) we have

$$P'_-(x_0) = \frac{x'_1(t)}{x'_0(t)} = -\frac{\Psi_{\lambda_1,\lambda_2}(t)}{\Psi_{\lambda_1,\lambda_2}(-t)} < 0. \tag{26}$$

Thus P_- is decreasing with respect to x_0 with a domain given by $(0, \frac{\lambda_2}{n})$ and has $x_0 = \frac{\lambda_2}{n}$ as an asymptote. Direct calculation from (25) gives

$$P''_-(x_0) = \frac{x'_0x''_1 - x''_0x'_1}{(x'_0)^3} = -\frac{n^2e^{-2mt}}{\lambda_1 - \lambda_2} \cdot \left[\frac{e^{\lambda_1t} - e^{\lambda_2t}}{\Psi_{\lambda_1,\lambda_2}(-t)} \right]^3 \cdot \sigma(t),$$

where $\sigma(t) = e^{mt} \cdot \Psi_{\lambda_1,\lambda_2}(-t) - \Psi_{\lambda_1,\lambda_2}(t)$. Then $\sigma'(t) = me^{mt} \cdot \Psi_{\lambda_1,\lambda_2}(-t) > 0$. So $P''_-(x_0) < 0$, and P_- is convex with respect to x_0 .

(3) When $0 > \lambda_1 > \lambda_2$, by (24), we know that

$$\lim_{t \rightarrow 0^+} x_0(t) = \lim_{t \rightarrow 0^+} x_1(t) = 0, \quad \lim_{t \rightarrow +\infty} x_0(t) = -\infty, \quad \lim_{t \rightarrow +\infty} x_1(t) = \frac{\lambda_1}{n}.$$

Thus, the domain of P_- is $(0, +\infty)$ and the asymptote is $x_1 = \frac{\lambda_1}{n}$. Since $m < 0$, similarly we have $P'_-(x_0) = -\frac{\Psi_{\lambda_1,\lambda_2}(t)}{\Psi_{\lambda_1,\lambda_2}(-t)} < 0$, $\text{sign}P''_- = -\text{sign}m$, $P''_-(x_0) > 0$. So P_- is decreasing and concave with respect to x_0 .

(4) According to the analysis given in proving statement (2), the continuity of P_- at the point $x_0 = 0$ is obvious. Using an approach similar to that in [18], we obtain

$$P_-(x_0) = -x_0 - \frac{2}{3}mx_0^2 - \frac{4}{9}m^2x_0^3 - \frac{2}{135}(22m^3 - 9mn)x_0^4 + o(x_0^4).$$

Finally we have the first four derivatives of P_- at this point.

Figure 4 shows phase portraits of the lower system of (3) when $\lambda_1 > \lambda_2 > 0$ and $0 > \lambda_1 > \lambda_2$, respectively. The domain of P_- is $(0, \frac{\lambda_2}{n})$ ($(0, +\infty)$) and the range of P_- is $(-\infty, 0)$ ($(\frac{\lambda_1}{n}, 0)$) when $\lambda_1 > \lambda_2 > 0$ ($0 > \lambda_1 > \lambda_2$).

Theorem 3 *Suppose that system (3) satisfies $m^2 > 4n > 0$ and $l < 0$. Then the following statements hold.*

- (1) *If $m < 0$, system (3) has no periodic orbit.*
- (2) *If $m > 0$ (that is, $\lambda_1 > \lambda_2 > 0$), $-\frac{n}{3\lambda_2} \leq l < 0$, system (3) has no periodic orbit.*
- (3) *If $m > 0$ (that is, $\lambda_1 > \lambda_2 > 0$), $-\frac{2m}{3} < l < -\frac{n}{3\lambda_2}$, there exist l_1, l_2 satisfying $-\frac{2m}{3} < l_1 < l_2 < -\frac{n}{3\lambda_2}$ such that the following statements hold.*
 - (a) *If $-\frac{2m}{3} < l < l_1$, system (3) has a stable limit cycle.*
 - (b) *If $l = l_1$, system (3) has a stable crossing critical cycle.*

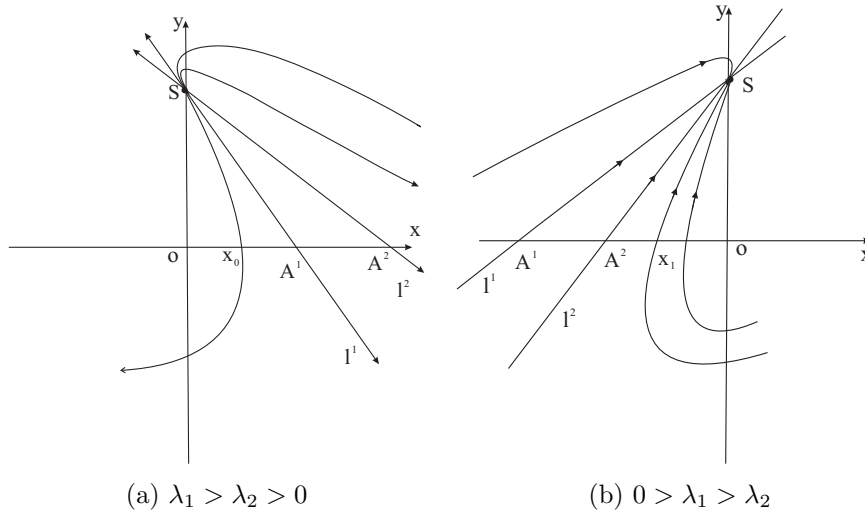


Figure 4: Phase portraits of lower system of (3)

- (c) If $l_1 < l < l_2$, system (3) has a stable sliding cycle.
 - (d) If $l = l_2$, system (3) has a sliding homoclinic cycle, which is stable.
 - (e) If $l_2 < l < -\frac{n}{3\lambda_2}$, system (3) has no periodic orbit.
- (4) If $m > 0$ (that is, $\lambda_1 > \lambda_2 > 0$), $l \leq -\frac{2m}{3}$, there are no corresponding l_1, l_2 that satisfy $-\infty < l_1 < l_2 < -\frac{2m}{3}$. So system (3) has no periodic orbit.

Theorem 4 Suppose that system (3) satisfies $m^2 > 4n > 0$, $l > 0$. Then the following statements hold.

- (1) If $m > 0$, system (3) has no periodic orbit.
- (2) If $m < 0$ (that is, $0 > \lambda_1 > \lambda_2$), $0 < l \leq -\frac{n}{3\lambda_2}$, system (3) has no periodic orbit.
- (3) If $m < 0$ (that is, $0 > \lambda_1 > \lambda_2$), $-\frac{n}{3\lambda_2} < l < -\frac{2m}{3}$, then there exist l_1, l_2 satisfying $-\frac{n}{3\lambda_2} < l_2 < l_1 < -\frac{2m}{3}$ such that the following statements hold:
 - (a) If $l_1 < l < -\frac{2m}{3}$, system (3) has an unstable limit cycle (crossing periodic orbit).
 - (b) If $l = l_1$, system (3) has an unstable crossing critical cycle.
 - (c) If $l_2 < l < l_1$, system (3) has an unstable sliding cycle.
 - (d) If $l = l_2$, system (3) has a sliding homoclinic cycle, which is unstable.
 - (e) If $-\frac{n}{3\lambda_2} < l < l_2$, system (3) has no periodic orbit.
- (4) If $m < 0$ (that is, $0 > \lambda_1 > \lambda_2$), $l \geq -\frac{2m}{3}$, then there are no corresponding l_1, l_2 that satisfy $-\frac{2m}{3} < l_2 < l_1 < +\infty$. So system (3) has no periodic orbit.

2.4 Hopf bifurcation

From [6, 15, 22] we know planar piecewise smooth system will undergo Hopf bifurcation near singular points of focus-focus (F-F) type, focus-parabolic (F-P) type, parabolic-parabolic (P-P) type. When the linear system has a focus, the origin of system (1) is a pseudo-focus of P-P type. We have the following results.

Theorem 5 Assume that $n > \frac{m^2}{4}$, $l < 0$, the following statements hold.

(i) If $l + \frac{2m}{3} < 0$ and $\epsilon_1 = 2\epsilon_2 - 3l\epsilon_2^2$ hold, then for $0 < \epsilon_2 \ll 1$, the P-P focus P_ϵ of system (2) is asymptotically stable.

(ii) If $l + \frac{2m}{3} = 0$, the origin of system (3) is an asymptotically stable pseudo-focus of order 4.

(iii) If $-\frac{2m}{3} < l < l_1$ and $\epsilon_1 = 2\epsilon_2 - 3l\epsilon_2^2$ hold, then for $0 < \epsilon_2 \ll 1$, the P-P focus P_ϵ of system (2) is unstable. Moreover, system (2) has a stable limit cycle and an unstable limit cycle if $\epsilon_1 > 2\epsilon_2 - 3l\epsilon_2^2$ and $0 < \epsilon_2 \ll 1$.

Theorem 6 Assume that $n > \frac{m^2}{4}$ and $l > 0$, the following statements hold.

(i) If $l + \frac{2m}{3} > 0$ and $\epsilon_1 = 2\epsilon_2 - 3l\epsilon_2^2$ hold, then for $0 < -\epsilon_2 \ll 1$, the P-P focus P_ϵ of system (2) is unstable.

(ii) If $l + \frac{2m}{3} = 0$, the origin of system (3) is an unstable pseudo-focus of order 4.

(iii) If $-\frac{2m}{3} > l > l_1$ and $\epsilon_1 = 2\epsilon_2 - 3l\epsilon_2^2$ hold, then for $0 < \epsilon_2 \ll 1$, the P-P focus P_ϵ of system (2) is asymptotically stable. Moreover, system (2) has an unstable limit cycle and a stable limit cycle if $\epsilon_1 < 2\epsilon_2 - 3l\epsilon_2^2$ and $0 < -\epsilon_2 \ll 1$.

From the above two theorems, we find that Hopf Bifurcation and critical crossing bifurcation occur. If $l > 0$, we shall have similar results. When the linear system has a node, the origin of system (1) is a pseudo-focus of P-P type. We have similar bifurcation phenomena.

3 Proof of the Main Results

In this section, we will prove our main results.

We recall some results in [22]. The equilibrium point of linear system is a saddle.

The eigenvalues of $A = \begin{pmatrix} m & n \\ -1 & 0 \end{pmatrix}$ are the following λ_1 and λ_2 . Other notations in the following proposition have similar meanings with Proposition 5.

Proposition 6 Suppose that system (5) satisfies the assumptions $n < 0$, $m \in R$ and $\lambda_1 > 0 > \lambda_2$, then the following statements hold.

(1) $x_0(t)$ is increasing with respect to t and $x_1(t)$ is decreasing with respect to t ,

$$\lim_{t \rightarrow 0^+} x_0(t) = \lim_{t \rightarrow 0^+} x_1(t) = 0, \quad \lim_{t \rightarrow \infty} x_0(t) = \frac{\lambda_2}{n}, \quad \lim_{t \rightarrow \infty} x_1(t) = \frac{\lambda_1}{n}.$$

(2) P_- is decreasing with respect to x_0 , P_- is concave (convex) when $m < 0$ ($m > 0$).

(3) When $m = 0$, $P_-(x_0) = -x_0$, where $x_0 \in (0, \frac{\lambda_2}{n})$.

(4) Define $P_-(0) = 0$, then P_- is continuous at the point $x_0 = 0$. In addition to this, the first four derivatives of the P_- at the point $x_0 = 0$ are

$$P'_-(0) = -1, \quad P''_-(0) = -\frac{4m}{3}, \quad P'''_-(0) = -\frac{8}{3}m^2, \quad P^{(4)}_-(0) = -\frac{16}{45}(22m^3 - 9mn).$$

Remark 1 Easy calculation shows that the process of obtaining $P_-(x_0)$ has nothing to do with the sign of n and the fact that whether λ_1, λ_2 are real roots or not, it follows that $P_-(x_0)$ still has the above expression in the case of focus. Moreover, direct calculation shows that the inverse of $P_-(x_0)$ has the following expression

$$P_-^{-1}(x_0) = -x_0 - \frac{2}{3}mx_0^2 - \frac{4}{9}m^2x_0^3 - \frac{2}{135}(22m^3 - 9mn)x_0^4 + o((-x_0)^4).$$

The graph of $P_-(x_0)$ is similar to that of $P_-^{-1}(x_0)$.

3.1 Proof of Theorem 1

(1) By Proposition 1, $P_+(x_0)$ is convex and decreasing with respect to x_0 when $l < 0$. Since $P'_+(0) = -1$, $P_+(x_0) < -x_0$ for all $x_0 \in (x_B, 0)$. By Proposition 2, $P_-^{-1}(x_0) \geq -x_0$ for $x_0 \in (-\infty, 0)$ when $m \leq 0$. Then

$$P_+(x_0) < P_-^{-1}(x_0), \quad x_0 \in (x_B, 0).$$

It means that the graphs of P_+ and P_-^{-1} have no intersection point, thus system (3) has no periodic orbit.

(2) By Proposition 2, x_0 is increasing with respect to s for $s \in (0, \pi)$

$$\lim_{s \rightarrow 0^+} x_0(s) = 0, \quad \lim_{s \rightarrow \pi^-} x_0(s) = +\infty.$$

For a given $l < 0$, there exists a unique $s_0 \in (0, \pi)$ such that

$$-\frac{1}{3l} = \frac{\beta}{n \sin s_0} [e^{-m\gamma s_0} - (\cos s_0 - m\gamma \sin s_0)]. \tag{27}$$

System (3) has a critical crossing cycle which is equivalent to there exists an $s_0 \in (0, \pi)$ such that $x_0(s_0, m) = -\frac{1}{3l}$ and $x_1(s_0, m) = \frac{2}{3l}$, that is $2x_0(s_0, m) + x_1(s_0, m) = 0$. Note that l is unknown, we should determine s_0 . By (19), we have

$$2e^{-m\gamma s_0}\varphi_{m\gamma}(s_0) - e^{m\gamma s_0}\varphi_{-m\gamma}(s_0) = 0. \tag{28}$$

It follows that

$$2e^{-m\gamma s_0} - \cos s_0 + 3m\gamma \sin s_0 - e^{m\gamma s_0} = 0. \tag{29}$$

Actually, in this case s_0 is independent of l . We will give a graph to show that for suitable values of $k = m\gamma > 0$, indeed there exists an $s_0 \in (0, \pi)$ such that equation (29) holds. With the help of computer, we know there exists an $s_0 \in (0, \pi)$ such that the equation holds for suitable values of $k > 0$. See Figure 5.

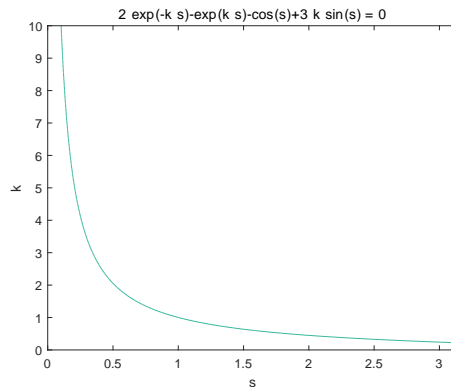


Figure 5: The graph of the function in equation (29)

Set

$$l_1 = -\frac{n \sin s_0}{3\beta[e^{-m\gamma s_0} - (\cos s_0 - m\gamma \sin s_0)]} < 0. \tag{30}$$

If $l = l_1$, then $x_1(s_0, m) = \frac{2}{3l}$, thus system (3) exists a critical crossing cycle.

If there exists an $s_1 \in (0, \pi)$ such that $x_0(s_1, m) = -\frac{1}{3l}$ and $x_1(s_1, m) = x_M^-$, then system (3) will have a sliding homoclinic cycle. Therefore, we need the following equations

$$\begin{aligned} x_0(s_1, m) &= \frac{\beta}{n \sin s_1} [e^{-m\gamma s_1} - (\cos s_1 - m\gamma \sin s_1)] = -\frac{1}{3l}, \\ x_1(s_1, m) &= -\frac{\beta}{n \sin s_1} [e^{m\gamma s_1} - (\cos s_1 + m\gamma \sin s_1)] \\ &= \frac{3l + 2m + \sqrt{(3l + 2m)^2 - 36lm}}{6lm}. \end{aligned}$$

We eliminate l from the above two equations and note that $l < 0$, we have the following equation

$$\frac{2m\gamma T}{\sin s_1(1 + m^2\gamma^2)} + e^{m\gamma s_1} - 3e^{-m\gamma s_1} + 2 \cos s_1 - 4m\gamma \sin s_1 = 0, \tag{31}$$

where $T = (e^{m\gamma s_1} - e^{-m\gamma s_1} - 2m\gamma \sin s_1)^2 - (e^{-m\gamma s_1} - \cos s_1 + m\gamma \sin s_1)^2$. Analogously, s_1 is independent of l . There are suitable values $k = m\gamma > 0$, indeed there exists an s_1 such that equation (31) holds. Since it is not easy to solve equation (31), in what follows we will give another graph to show there exists an $s_1 \in (0, \pi)$ such that equation (31) holds. Let $k = m\gamma > 0$, then we have the following equation

$$\begin{aligned} \frac{2k}{\sin s_1(1 + k^2)} [(e^{ks_1} - e^{-ks_1} - 2k \sin s_1)^2 - (e^{-ks_1} - \cos s_1 + k \sin s_1)^2] \\ + e^{ks_1} - 3e^{-ks_1} + 2 \cos s_1 - 4k \sin s_1 = 0. \end{aligned}$$

With the help of Matlab, we have Figure 6. It shows that there exists an $s_1 \in (0, \pi)$ such that the equation holds for suitable values of $k > 0$.

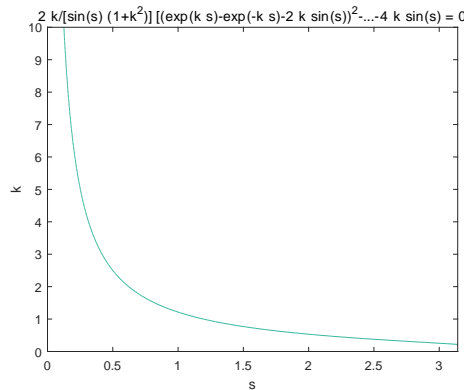


Figure 6: The graph of the function in equation (31)

Set

$$l_2 = -\frac{n \sin s_1}{3\beta[e^{-m\gamma s_1} - (\cos s_1 - m\gamma \sin s_1)]} < 0.$$

If $l = l_2$, then $x_1(s_0, m) = \frac{2}{3l}$, thus system (3) exists a sliding homoclinic cycle.

From Proposition 1 and the above remark, we have

$$\begin{aligned} P_+(x_0) - P_-^{-1}(x_0) &= \left(l + \frac{2}{3}m\right)x_0^2 + \left(\frac{4}{9}m^2 - l^2\right)x_0^3 \\ &\quad + \left(2l^3 + \frac{2}{135}(22m^3 - 9mn)\right)x_0^4 + o((-x_0)^4), \end{aligned} \quad (32)$$

where $-x_0 > 0$ is small enough.

If $l > -\frac{2}{3}m$, then $P_+(x_0) - P_-^{-1}(x_0) > 0$ when $-x_0 > 0$ is small enough. Suppose that lower orbits starting at the point \bar{B} will arrive Σ again at the point C . From $x_0(s, m) = -\frac{1}{3l}$ and $\frac{dx_1}{dl} = \frac{dx_1}{ds} \frac{ds}{dl}$, we have the following derivative of x_1 with respect to l ,

$$\begin{aligned} \frac{dx_1}{dl} &= -\frac{\beta(1+m\gamma \sin s \cdot e^{m\gamma s} - \cos s \cdot e^{m\gamma s})}{n(\sin s)^2} \cdot \frac{n(\sin s)^2}{3l^2\beta(1-m\gamma \sin s \cdot e^{-m\gamma s} - \cos s \cdot e^{-m\gamma s})} \\ &= -\frac{\varphi_{m\gamma}(s)}{3l^2\varphi_{-m\gamma}(s)}, \end{aligned}$$

where $\gamma = \frac{1}{\sqrt{4n-m^2}}$. Note that $m\gamma > 0$, we obtain $\frac{dx_1}{dl} < 0$. Furthermore, note that $x_{M^-} < x_B$, x_1 is decreasing with respect to s , then $s_1 > s_0$. Since $\frac{ds}{dl} > 0$, we have $l_2 > l_1$.

Therefore, if $-\frac{2}{3}m < l < l_1$, then $x_1(s, m) > \frac{2}{3l}$. We conclude from Proposition 2 that

$$\lim_{x_0 \rightarrow 0^+} P'_-(x_0) = -1, \quad P''_-(x_0) < 0.$$

Then we have $P_-(x_0) < -x_0$ and $x_C < \frac{1}{3l}$, where x_C is the abscissa of the point C . It follows that

$$\frac{2}{3l} < x_1(s, m) < \frac{1}{3l}.$$

This means that C is always on the right of B . Moreover, $P_-^{-1}(x_B) > x_{\bar{B}} = P_+(x_B)$. Using the monotonicity and concave properties of P_+ , P_-^{-1} , there exists a unique $x_0^1 \in (\frac{2}{3l}, 0)$ such that $P_-^{-1}(x_0^1) = P_+(x_0^1)$, and

$$\begin{aligned} P_+(x_0) &> P_-^{-1}(x_0), \quad x_0 \in (x_0^1, 0), \\ P_+(x_0) &< P_-^{-1}(x_0), \quad x_0 \in \left(\frac{2}{3l}, x_0^1\right). \end{aligned}$$

Hence system (3) has a stable limit cycle (crossing periodic orbit), see Figure 7(a).

If $l = l_1$, then

$$x_1(s, m) = \frac{2}{3l}.$$

This means that C coincides with B . System (3) has a stable crossing critical cycle, see Figure 7(b).

If $l_1 < l < l_2$, we have $x_M^- < x_1(s, m) < \frac{2}{3l}$. This means that C is in the sliding region Σ_s^- and is located between M^- and B . Based on the analysis about the sliding vector field Y_s , we see that the orbits arriving at Σ_s^- and between M^- and B will turn right and move to B along Σ_s^- . Therefore, there exists a sliding cycle. Moreover, it also implies that $P_-^{-1}(x_B) < x_{\bar{B}} = P_+(x_B)$. The monotonicity and concave properties of P_+ , P_-^{-1} imply that

$$P_+(x_0) > P_-^{-1}(x_0), \quad x_0 \in \left(\frac{2}{3l}, 0\right),$$

when $x_0 \in (x_C, \frac{2}{3l})$ and $x_0 \in (x_M^-, x_C)$, the lower orbits will arrive at Σ_s^- and finally coincide with the sliding cycle when time is large enough. It means that system (3) has a stable sliding cycle, see Figure 7(c).

If $l = l_2$, then

$$x_1(s, m) = x_M^-.$$

This means that C coincides with M^- . The sliding homoclinic cycle is stable, see Figure 7(d).

If $l_2 < l < 0$, then $x_1(s, m) < x_M^-$. This means that C is always on the left of M^- . Based on the analysis about the sliding vector field Y_s , the orbits arriving at certain points which are located on the left of M^- will turn left and move to $-\infty$ along Σ_s^- . Therefore, system (3) has neither periodic orbits nor sliding cycles, see Figure 7(e).

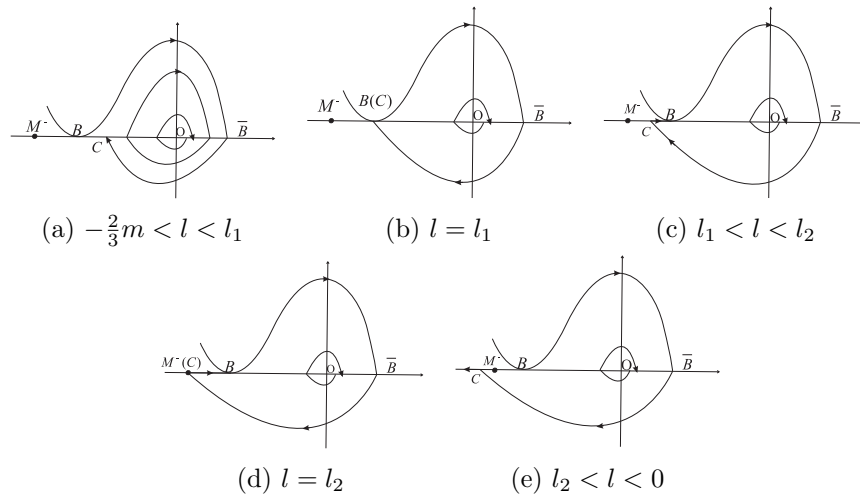


Figure 7: The topological structures of trajectories in (3) of Theorem 1

(3) We prove this part by contradiction. If there are l_1, l_2 that satisfy $-\infty < l_1 < l_2 < -\frac{2}{3}m$. That is, when $m > 0, l \leq -\frac{2}{3}m$, the orbit of the lower system will coincide with the orbit of upper system that starts from the point B to the point

M^- on Σ . So system (3) has a periodic orbit in this case. Moreover, system (3) will undergo critical crossing bifurcation CC_2 . However, according to the result in [12], critical crossing bifurcation CC_2 will not occur. We reach a contradiction.

Remark 2 In this case, when $l = l_1$, system (3) will undergo critical crossing bifurcation CC . When $l = l_2$, system (3) will undergo pseudo-homoclinic bifurcation. The homoclinic loop will pass through the pseudo-saddle M^- .

Remark 3 Notice that if we let $x \rightarrow -x, y \rightarrow y, t \rightarrow -t, m \rightarrow -m, l \rightarrow -l$ and $n \rightarrow n$, system (3) is invariant. So Theorem 2 is a direct consequence of Theorem 1.

Remark 4 In Theorem 2 it should be noted that if $l > 0$, then $x_{M^+} > x_B > 0$. x_1 is decreasing with respect to s , s is increasing with respect to l , so $s_1 < s_0$ and $l_2 < l_1$. Although we have use the same notations l_1 and l_2 in our main results, we have illustrated l_1 and l_2 in the proof of related theorems. Thus we should not confuse them.

3.2 Proof of Theorem 3

(1). Suppose that $l < 0$, by Proposition 1, we have $P_+(x_0) < -x_0$ for all $x_0 \in (x_B, 0)$. By Proposition 5, $P_-^{-1}(x_0) > -x_0$ for $x_0 \in (-\infty, 0)$ when $m < 0$. Then

$$P_+(x_0) < P_-^{-1}(x_0), \quad x_0 \in (x_B, 0).$$

It means that the graphs of P_+ and P_-^{-1} have no intersection point, thus system (3) has no periodic orbit when $l < 0$ and $m < 0$.

(2) Suppose that $m > 0$ and $-\frac{n}{3\lambda_2} \leq l < 0$. It follows that

$$\frac{\lambda_2}{n} = \frac{m - \sqrt{m^2 - 4n}}{2n} \leq -\frac{1}{3l}.$$

This is $x_{A^1} \leq x_{\bar{B}}$. In this case, $P_+(\frac{2}{3l}) > P_-^{-1}(\frac{2}{3l})$. In fact, $P_+(\frac{2}{3l}) = -\frac{1}{3l} \geq \frac{\lambda_2}{n} > P_-^{-1}(\frac{2}{3l})$. It is not difficult to check that $-\frac{n}{3\lambda_2} = -\frac{\lambda_1}{3} > -\frac{2m}{3} = -\frac{2(\lambda_1 + \lambda_2)}{3}$. So $l > -\frac{2m}{3}$. By (32), $P_+(x_0) > P_-^{-1}(x_0)$ when $-x_0 > 0$ is small enough. The monotonicity and concave properties of P_+, P_-^{-1} imply that

$$P_+(x_0) > P_-^{-1}(x_0), \quad x_0 \in \left(\frac{2}{3l}, 0\right).$$

Then the graphs of P_+ and P_-^{-1} have no intersection point and system (3) has no periodic orbit.

(3) Suppose that $m > 0$ and $l < -\frac{n}{3\lambda_2}$. We conclude that $-\frac{1}{3l} = x_{\bar{B}} < \frac{n}{\lambda_2} = x_{A^1}$ and $-\frac{1}{3l}$ is in the domain of x_0 . Using the monotonicity of $x_0(t)$, there exists a unique $t \in (0, +\infty)$ such that

$$x_0(t) = \frac{1}{n} \cdot \frac{\Psi_{\lambda_1, \lambda_2}(t)}{e^{\lambda_1 t} - e^{\lambda_2 t}} = -\frac{1}{3l}.$$

System (3) has a critical crossing cycle which is equivalent to there exist a $t_0 > 0$ and a constant $l_1 < 0$ such that $x_0(t_0) = -\frac{1}{3l_1}$ and $x_1(t_0) = \frac{2}{3l_1}$. That is

$$e^{mt_0}\Psi_{\lambda_1,\lambda_2}(-t_0) - 2\Psi_{\lambda_1,\lambda_2}(t_0) = 0. \tag{33}$$

This implies that t_0 is independent of l . In the next section, we will give some examples to show that for suitable values of m, n , there exists a t_0 such that equation (33) holds. Set

$$l_1 = -\frac{n(e^{\lambda_1 t_0} - e^{\lambda_2 t_0})}{3\Psi_{\lambda_1,\lambda_2}(t_0)} < 0. \tag{34}$$

If $l = l_1$, then $x_1(t_0) = \frac{2}{3l}$, system (3) has a critical crossing cycle.

Moreover, by Proposition 5, it is easy to know that $x_1(t)$ is decreasing with respect to l ,

$$\lim_{l \rightarrow -\frac{n}{3\lambda_2}} x_1(t) = \lim_{x_0(t) \rightarrow \frac{n}{\lambda_2}} x_1(t) = -\infty, \quad \lim_{l \rightarrow -\infty} x_1(t) = \lim_{x_0(t) \rightarrow 0} x_1(t) = 0. \tag{35}$$

So there exist a unique $t = t_0$ and a constant l_1 satisfying $-\infty < l_1 < -\frac{n}{3\lambda_2}$ such that $x_0(t_0) = -\frac{1}{3l_1}$ and $x_1(t_0) = \frac{2}{3l_1}$.

System (3) will have a sliding homoclinic cycle if there exist a $t_1 > 0$ and a constant l_2 such that $x_0(t_1) = -\frac{1}{3l_2}$ and $x_1(t_1, l_2) = x_M^-$. Analogously, we eliminate l from the above two equations, we have

$$me^{mt_1}\Psi_{\lambda_1,\lambda_2}(-t_1)[e^{mt_1}\Psi_{\lambda_1,\lambda_2}(-t_1) - 2\Psi_{\lambda_1,\lambda_2}(t_1)] + n(e^{\lambda_1 t_1} - e^{\lambda_2 t_1})[e^{mt_1}\Psi_{\lambda_1,\lambda_2}(-t_1) - 3\Psi_{\lambda_1,\lambda_2}(t_1)] = 0. \tag{36}$$

Then t_1 is independent of l . There are suitable values m and n such that the above equation holds. The monotonicity of $x_1(t)$ with respect to l verifies our results. Set

$$l_2 = -\frac{n(e^{\lambda_1 t_1} - e^{\lambda_2 t_1})}{3\Psi_{\lambda_1,\lambda_2}(t_1)} < 0. \tag{37}$$

If $l = l_2$, then $x_1(t_1) = \frac{2}{3l}$, system (3) exists a sliding homoclinic cycle. Using the monotonicity, we know that $0 < t_0 < t_1$, $-\infty < l_1 < l_2 < -\frac{n}{3\lambda_2}$. The remaining proof of each condition for l can be discussed similarly as the statement of Theorem 1. Here we omit it.

(4) The proof is similar to that of case (3) in Theorem 1. Notice

$$l_1 = -\frac{\lambda_1\lambda_2(e^{\lambda_1 t_0} - e^{\lambda_2 t_0})}{3\Phi_{\lambda_1,\lambda_2}(t_0)} = -\frac{2}{3}m \cdot \frac{\lambda_1\lambda_2(e^{\lambda_1 t_0} - e^{\lambda_2 t_0})}{2(\lambda_1 + \lambda_2)\Phi_{\lambda_1,\lambda_2}(t_0)}, \tag{38}$$

we take the objective function

$$f(t_0, \lambda_1, \lambda_2) = \lambda_1\lambda_2(e^{\lambda_1 t_0} - e^{\lambda_2 t_0}) - 2(\lambda_1 + \lambda_2)(\lambda_1 - \lambda_2 + \lambda_2 e^{\lambda_1 t_0} - \lambda_1 e^{\lambda_2 t_0}). \tag{39}$$

Under the constraint of equation (33), when $t_0 = \lambda_1 = \lambda_2 = 0$, the objective function $f(t_0, \lambda_1, \lambda_2)$ gets the maximum value of 0 with the help of Matlab. Therefore, when $t_0 > 0$, $\lambda_1 > \lambda_2 > 0$, the value of $f(t_0, \lambda_1, \lambda_2)$ is less than 0. That is

$$\frac{\lambda_1\lambda_2(e^{\lambda_1 t_0} - e^{\lambda_2 t_0})}{2(\lambda_1 + \lambda_2)\Phi_{\lambda_1,\lambda_2}(t_0)} < 1, \tag{40}$$

so it is always true that $l_1 > -\frac{2}{3}m$.

For l_2 , if we take the same objective function, we will get the same result under the constraint of equation (36) as in the case of l_1 . That is, when $t_1 = \lambda_1 = \lambda_2 = 0$, the objective function $f(t_1, \lambda_1, \lambda_2)$ gets the maximum value of 0. Similarly, it is always true that $l_2 > -\frac{2}{3}m$.

To sum up, there is no corresponding l_1, l_2 that satisfy $-\infty < l_1 < l_2 < -\frac{2}{3}m$. That is, when $m > 0, l \leq -\frac{2}{3}m$, system (3) has no periodic orbit.

Remark 5 Similarly, if we let $x \rightarrow -x, y \rightarrow y, t \rightarrow -t, m \rightarrow -m, l \rightarrow -l$ and $n \rightarrow n$, system (3) is invariant. This shows that system (3) has the symmetry property, so Theorem 4 is a direct consequence of Theorem 3. In what follows we give main topological structures of trajectories in (3) of Theorem 4. We need to notice that there exists a pseudo-saddle M^+ in the repulsive sliding region Σ_s^+ , see Proposition 4.

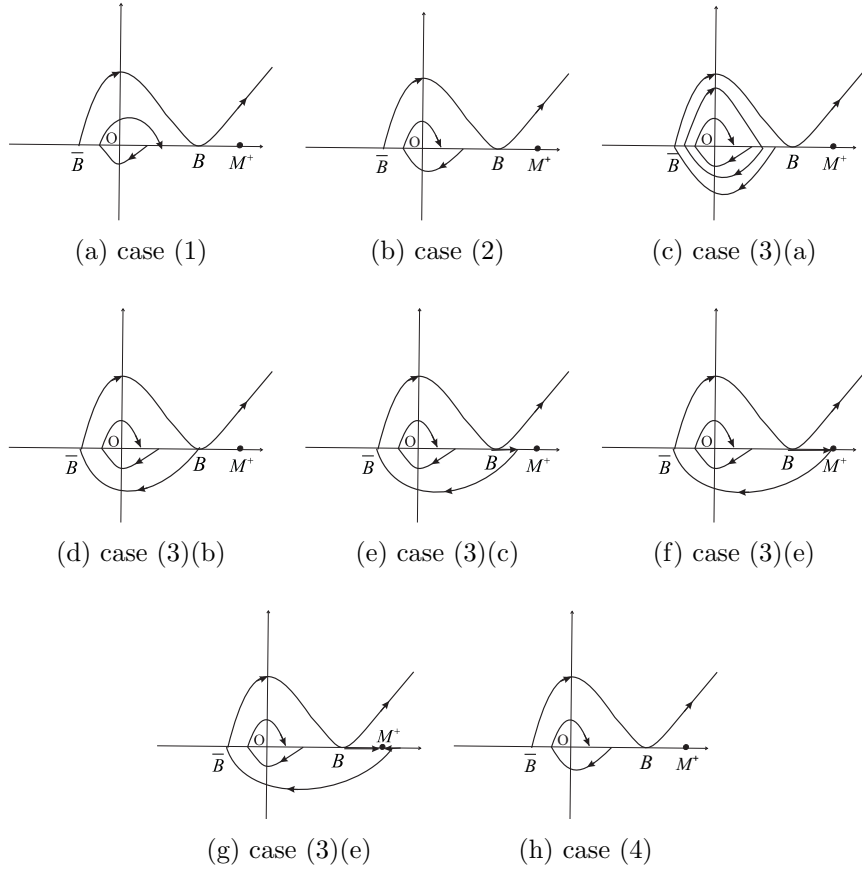


Figure 8: The topological structures of trajectories in (3) of Theorem 4

3.3 Proof of Theorem 5

In this part, we shall discuss the existence of Hopf bifurcation. We shall prove Theorem 5. The main ideas are from [22].

(i) Denote by $P_\epsilon^+ = (\frac{1-\sqrt{1-3l\epsilon_1}}{3l}, 0)$, $P_\epsilon^- = (\epsilon_2, 0)$. We know that if $\epsilon_1 = 2\epsilon_2 - 3l\epsilon_2^2$, P_ϵ^+ coincides with P_ϵ^- as one point P_ϵ . P_ϵ has the same stability as $O(0,0)$ for the same reason as we can find in [22]. For $-x_0 > 0$ sufficiently small, we get from (32) that if $l + \frac{2m}{3} > 0$, we have $P_+(x_0) - P_-^{-1}(x_0) > 0$. If $l + \frac{2m}{3} < 0$, we have $P_+(x_0) - P_-^{-1}(x_0) < 0$. This shows that $O(0,0)$ is asymptotically stable if $l + \frac{2m}{3} < 0$ and $O(0,0)$ is unstable if $l + \frac{2m}{3} > 0$.

(ii) If $l + \frac{2m}{3} = 0$, it follows from (32) that

$$\begin{aligned} P_+(x_0) - P_-^{-1}(x_0) &= \left[2l^3 + \frac{2(22m^3 - 9mn)}{135} \right] x_0^4 + o((-x_0^4)) \\ &= -\frac{18m(n + 2m^2)}{135} x_0^4 + o((-x_0^4)). \end{aligned}$$

Notice that when the linear system has a focus, we have $n > \frac{m^2}{4} > 0$. We get $-\frac{18m(n+2m^2)}{135} > 0$ if $m < 0$ and $-\frac{18m(n+2m^2)}{135} < 0$ if $m > 0$. We conclude that the origin $O(0,0)$ is a focus of 4th order. Since $l + \frac{2m}{3} = 0$, the origin $O(0,0)$ is unstable if $l > 0$ and it is asymptotically stable if $l < 0$.

(iii) Under the assumptions, Hopf bifurcation occurs similarly to [22]. Hence we shall get a limit cycle from Hopf bifurcation. For the unperturbed system (3), there exists a limit cycle due to critical crossing bifurcation. Since this limit cycle is stable or unstable, it is hyperbolic. Hence it will persist under small perturbation. Finally, system (2) has two limit cycles with different stability in total. Theorem 6 can be proved similarly.

4 Some Examples

In this section, we will give some examples to show that the conditions in Theorems 1 and 3 hold.

Example 1 Let $m = 1$, $n = \frac{5}{4}$, then $n > \frac{m^2}{4}$, $\beta = \frac{\sqrt{4n-m^2}}{2} = 1$, $\gamma = \frac{1}{2\beta} = \frac{1}{2}$, $k = m\gamma = \frac{1}{2}$. (29) is rewritten as

$$2e^{-\frac{s_0}{2}} - \cos s_0 + \frac{3}{2} \sin s_0 - e^{\frac{s_0}{2}} = 0. \quad (41)$$

There is a unique root $s_0 \approx 1.84$ for equation (41). It follows that $l_1 \approx -0.35$. Therefore, we have $l_1 > -\frac{2m}{3}$.

For $k = m\gamma = \frac{1}{2}$, equation (31) is rewritten as

$$\begin{aligned} &\frac{1}{\frac{5}{4} \sin s_1} \left[(e^{\frac{1}{2}s_1} - e^{-\frac{1}{2}s_1} - \sin s_1)^2 - \left(e^{-\frac{1}{2}s_1} - \cos s_1 + \frac{1}{2} \sin s_1 \right)^2 \right] \\ &+ e^{\frac{1}{2}s_1} - 3e^{-\frac{1}{2}s_1} + 2 \cos s_1 - 2 \sin s_1 = 0. \end{aligned} \quad (42)$$

Using Matlab, we get a unique root $s_1 \approx 2.09 \in (0, \pi)$ of equation (42). Moreover, $s_1 > s_0 \approx 1.84$. Now

$$l_2 = \frac{-n \sin s_1}{3\beta[(e^{-\frac{s_1}{2}}) - (\cos s_1 - \frac{1}{2} \sin s_1)]} \approx -0.28.$$

It follows that $0 > l_2 > l_1$.

Example 2 Let $m = 2, n = 2$, then $n > \frac{m^2}{4}, \beta = \frac{\sqrt{4n-m^2}}{2} = 1, \gamma = \frac{1}{2\beta} = \frac{1}{2}, k = m\gamma = 1$. Similarly, there is a unique root $s_0 \approx 1.00 \in (0, \pi)$ of equation (29). We have $l_1 \approx -0.84$. Equation (31) is

$$(e^{s_1} - e^{-s_1} - 2 \sin s_1)^2 - (e^{-s_1} - \cos s_1 + \sin s_1)^2 + e^{s_1} \sin s_1 - 3e^{-s_1} \sin s_1 + 2 \sin s_1 \cos s_1 - 4(\sin s_1)^2 = 0.$$

With the help of computer, we get a unique root $s_1 \approx 1.19$ for the above equation. Note that $l_2 \approx -0.72$, this means that $l_1 < l_2 < 0$ holds.

Example 3 Let $m = 5, n = 6, m^2 > 4n > 0$. Then $\lambda_1 = 3, \lambda_2 = 2, \lambda_1 > \lambda_2 > 0$, and $-\frac{n}{3\lambda_2} = -1$. Then (33) is

$$2 + 7e^{3t_0} - 8e^{2t_0} - e^{5t_0} = 0. \tag{43}$$

With the help of computer, we obtain a unique root $t_0 \approx 0.41 > 0$ for the above equation. Substituting t_0 into (34), we have $l_1 \approx -2.23$. (36) is

$$5(e^{5t_1} + 2e^{2t_1} - 3e^{3t_1})(8e^{2t_1} + e^{5t_1} - 7e^{3t_1} - 2) + 6(e^{3t_1} - e^{2t_1})(e^{5t_1} + 11e^{2t_1} - 9e^{3t_1} - 3) = 0. \tag{44}$$

With the help of computer, we obtain a unique root $t_1 \approx 0.51 > 0$ for the above equation (44). Substituting t_1 into (37), we have $l_2 \approx -1.92$. Indeed, we have $0 < t_0 < t_1, -\infty < l_1 < l_2 < -\frac{n}{3\lambda_2}$. It follows that $l_2 > l_1 > -\frac{2m}{3} \approx -3.33$.

Example 4 Let $m = 8, n = 15, m^2 > 4n > 0$. Then $\lambda_1 = 5, \lambda_2 = 3, \lambda_1 > \lambda_2 > 0$, and $-\frac{n}{3\lambda_2} = -\frac{5}{3}$. Then (33) is

$$4 - 13e^{3t_0} + 11e^{5t_0} - 2e^{8t_0} = 0. \tag{45}$$

With the help of computer, we obtain a unique root $t_0 \approx 0.26 > 0$ for the above equation. Substituting t_0 into (34), we have $l_1 \approx -3.54$. (36) is

$$8(2e^{8t_1} + 3e^{3t_1} - 5e^{5t_1})(2e^{8t_1} + 13e^{3t_1} - 11e^{5t_1} - 4) + 15(e^{5t_1} - e^{3t_1})(2e^{8t_1} + 18e^{3t_1} - 14e^{5t_1} - 6) = 0. \tag{46}$$

With the help of computer, we obtain a unique root $t_1 \approx 0.32 > 0$ for the above equation (46). Substituting t_1 into (37), we have $l_2 \approx -3.08$. Indeed, we have $0 < t_0 < t_1, -\infty < l_1 < l_2 < -\frac{n}{3\lambda_2}$. It follows that $l_2 > l_1 > -\frac{2m}{3} \approx -5.33$.

5 Conclusions

In this paper we provide a bifurcation analysis for a planar PWS system which consists of a quadratic Hamiltonian system and a linear system. If its linear system has a focus, we prove that PWS system (3) has a periodic orbit and a sliding cycle.

Moreover, PWS system (2) will have two limit cycles and undergo pseudo-homoclinic bifurcation and critical crossing bifurcation CC .

If the linear system has a node, we also find that this PWS system will have a sliding cycle and undergo pseudo-homoclinic bifurcation and critical crossing bifurcation CC . Although we have some similar bifurcation phenomena when the linear system has a focus or a node. As far as we know, the results that we see a sliding cycle in a PWS system with a node are new.

Compared with some existing works, although pseudo-homoclinic bifurcation and sliding cycle were mentioned in [14] and [21], we have only seen them in a PWS system whose subsystem has a focus (see e.g. [10, 13, 28, 29]). We don't see them in a piecewise smooth system whose subsystem has a node (see e.g. [18] and [27]). The first reason for there do not exist sliding phenomena in paper [18] is that the trajectories are controlled by the invariant straight lines of the two linear subsystems. Moreover, there does not exist a tangency point. A tangency point is usually an exit point for a sliding cycle. This implies that even if the trajectories slide on the discontinuity line, we cannot get a sliding cycle.

In [18], the authors did not find a sliding cycle. However, when the PWS system has a node, we have a sliding cycle. On one hand, our sliding set is an infinite interval. Our trajectories have more freedom. On the other hand, the upper quadratic system has a visible tangency point on the discontinuity line, which ensures that the orbits sliding on the discontinuity line can exit from there. Finally, our PWS system has a pseudo-saddle which is independent of the parameter n . These reasons improve the possibility of sliding phenomena, pseudo-homoclinic bifurcation and critical crossing cycle bifurcation CC .

Another thing we need mention is that as we can see from [11], when a subsystem of PWS system has a focus on the discontinuity line, three limit cycles can bifurcate from this PWS system, even if the subsystem is a linear system. Hence if we choose other perturbation such that the perturbed system has a focus on the discontinuity line, it is possible for this PWS to have three limit cycles.

Acknowledgements We would like to thank the referee for their valuable suggestions which improve the presentation of the paper.

References

- [1] A. Andronov, A. Vitt, S. Khaikin, Theory of Oscillations, Pergamon Press, Oxford, UK, 1966.
- [2] J.C. Artés, J. Llibre, Quadratic Hamiltonian vector fields, *J. Differential Equations*, **107**(1994),80-95.
- [3] C.A. Buzzi, P.R. da Silva, M.A. Teixeira, A singular approach to discontinuous vector fields on the plane, *J. Differential Equations*, **231**(2006),633-655.
- [4] C. Buzzi, T. de Carvalho, M.A. Teixeira, On 3-parameter families of piecewise smooth vector fields in the plane, *SIAM J. Appl. Dyn. Syst.*, **11**(2012),1402-1424.

- [5] S. Chen, Stability and perturbations of generalized heteroclinic loops in piecewise smooth systems, *Qual. Theory Dyn. Syst.*, **17**(2018),563-581.
- [6] B. Coll, A. Gasull, Degenerate Hopf bifurcation in discontinuous planar systems, *J. Math. Anal. Appl.*, **253**(2001),671-690.
- [7] M. di Bernardo, C.J. Budd, A.R. Champneys, P. Kowalczyk, Piecewise-smooth Dynamical Systems, Theory and Applications, Applied Mathematical Sciences **163**, Springer-Verlag, London, 2008.
- [8] L. Dieci, C. Elia, Periodic orbits for planar piecewise linear systems with a line of discontinuity, *J. Dyn. Differ. Equ.*, **26**(2014),1049-1078.
- [9] A.F. Filippov, Differential Equations with Discontinuous Right-hand Sides, Kluwer Academic Publishers, Dordrecht, 1988.
- [10] E. Freire, E. Ponce, F. Torres, Canonical discontinuous planar piecewise linear systems, *SIAM. J. Applied Dynam. Sys.*, **11**(2012),181-211.
- [11] E. Freire, E. Ponce, F. Torres, A general mechanism to generate three limit cycles in planar Filippov systems with two zones, *Nonlinear Dyn.*, **78**(2014),251-263.
- [12] E. Freire, E. Ponce, F. Torres, On the critical crossing cycle bifurcation in planar Filippov systems, *J. Differential Equations*, **259**(2015),7086-7107.
- [13] F. Gannakopoulos, K. Pliete, Planar systems of piecewise linear differential equations with a line of discontinuity, *Nonlinearity*, **14**(2001),1611-1632.
- [14] M. Guardia, T. Seara, M.A. Teixeira, Generic bifurcations of low codimension of planar Filippov systems, *J. Differential Equations*, **250**(2011),1967-2023.
- [15] M. Han, W. Zhang, On Hopf bifurcation in non-smooth planar systems, *J. Differential Equations*, **248**(2010),2399-2416.
- [16] C. Henry, Differential equation with discontinuous righthand side for planning procedure, *J. Econom. Theory*, **4**(1972),541-551.
- [17] S. Huan, X. Yang, Existence of limit cycles in general planar piecewise linear systems of saddle-saddle dynamics, *Nonlinear Anal.*, **92**(2013),82-95.
- [18] S. Huan, X. Yang, On the number of limit cycles in general planar piecewise linear systems of node-node types, *J. Math. Anal. Appl.*, **411**(2014),340-353.
- [19] Y. Ilyashenko, Centennial history of Hilbert's 16th problem, *Bull. Amer. Math. Soc. (N.S.)*, **39**(2002),301-354.
- [20] M. Kunze, T. Küpper, Qualitative bifurcation analysis of a non-smooth friction-oscillator model, *Z. Angew. Math. Phys.*, **48**(1997),87-101.
- [21] Y. Kuznetsov, S. Rinaldi, A. Gragnani, One-parametric bifurcations in planar Filippov systems, *Int. J. Bifur. Chaos.*, **13**(2003),2157-2188.
- [22] L. Li, L. Huang, Concurrent homoclinic bifurcation and Hopf bifurcation for a class of planar Filippov systems, *J. Math. Anal. Appl.*, **411**(2014),83-94.
- [23] J. Li, Hilbert's 16th problem and bifurcations of planar polynomial vector fields, *Int. J. Bifur. Chaos.*, **13**(2003),47-106.
- [24] F. Liang, M. Han, X. Zhang, Bifurcation of limit cycles from generalized homoclinic loops in planar piecewise smooth systems, *J. Differential Equations*, **255**(2013),4403-4436.

- [25] F. Liang, D. Wang, Limit cycle bifurcations near a piecewise smooth generalized homoclinic loop with a saddle-fold point, *Int. J. Bifur. Chaos.*, **27**(2017),1750071.
- [26] J. Llibre, E. Ponce, F. Torres, On the existence and uniqueness of limit cycles in Liénard differential equations allowing discontinuities, *Nonlinearity*, **21**(2008),2121-2142.
- [27] D. Pi, S. Xu, Bifurcation analysis of planar piecewise smooth systems with a line of discontinuity, *Int. J. Bifur. Chaos.*, **26**(2016),1650104.
- [28] D. Pi, J. Yu, X. Zhang, On the sliding bifurcation of a class of planar Filippov systems, *Int. J. Bifur. Chaos.*, **23**(2013),1350040.
- [29] D. Pi, X. Zhang, The sliding bifurcations in planar piecewise smooth differential systems, *J. Dyn. Differ. Equ.*, **25**(2013),1001-1026.
- [30] D. Simpson, Bifurcations in Piecewise-smooth Continuous Systems, World Scientific Series on Nonlinear Science, **69**, World Scientific, Singapore, 2010.
- [31] S. Tang, J. Liang, Y. Xiao, A. Robert, Sliding bifurcations of Filippov two stage pest control models with economic thresholds, *SIAM J. Appl. Math.*, **72**(2012),1061-1080.
- [32] J. Yang, L. Zhao, Bounding the number of limit cycles of discontinuous differential systems by using Picard-Fuchs equations, *J. Differential Equations*, **264**(2018),5734-5757.

(edited by Mengxin He)